NATIONAL TRANSPORTATION SAFETY BOARD

Office of Research and Engineering
Washington, D.C. 20594

April 9, 2001

Aircraft Performance - Addendum #4

Addendum to Group Chairman's Aircraft Performance Study
by John O'Callaghan

A. ACCIDENT

Location:	Sixty miles South of Nantucket, MA
Date:	October 31, 1999
Time:	0150 Eastern Standard Time (EST)
Flight:	EgyptAir Flight 990
Aircraft:	Boeing 767-366ER, Registration SU-GAP
NTSB#:	DCA00MA006

B. GROUP

Chairman: John O'Callaghan
Senior Aerospace Engineer
NTSB

Members: Mohamed A. Hamid Hamdy
Engineer - General Manager Training
EgyptAir

Maher Ismaiel Mohamed
Head of Airworthiness - Central Administration
Egyptian Civil Aviation Authority

Dennis D. Chandler
Engineer - PW4000 Operability/ Propulsion System Analysis
Pratt & Whitney

John Hed
Flight Test Engineer
Federal Aviation Administration

Timothy Mazzitelli
Lead Engineer - Aerodynamics, Stability & Control
The Boeing Company

C. SUMMARY

The wreckage of MSR990 was found in two debris fields about 1,200 feet apart. The main debris field, centered at 40° 20' 51" N, 69° 45' 24" W, contained the bulk of the airplane fuselage, wings, empennage, right engine, and flight recorders. A smaller debris field, centered at 40° 20' 57" N, 69° 45' 40" W, consisted mainly of parts associated with the left engine. This Addendum to the Aircraft Performance Group Chairman's Aircraft Performance Study presents the results of a calculation of the points at which an engine separating from MSR990 would impact the ocean surface, assuming various ballistic coefficients for the engine, and five different separation points along the MSR990 flight path. The calculations indicate that it is very unlikely that the left engine separated from MSR990 at or near the bottom of the first dive. Some of the engine impact points corresponding to an engine separation at 24,000 feet during the climb after the first dive are close to the debris field where the left engine parts were found, but the relatively low airspeed and normal load factor at this point (as determined from radar data) make it unlikely that the separation occurred here. No calculations were performed for separation points corresponding to the second and final dive of MSR990 because of the sparse and uncertain radar data during this time. However, the proximity of the airplane during the final dive to the debris fields and the high airspeeds that must have been encountered during this dive make it more likely that the engine separation occurred during this second dive, rather than before it.

D. DETAILS OF THE INVESTIGATION

An object separating from an airplane in flight will follow a ballistic trajectory determined by gravitational and aerodynamic forces. By definition, the only aerodynamic force acting on a "ballistic" body is drag, acting in a direction opposite that of the velocity vector of the object. In this study, it is assumed that the engine that separates from MSR990 behaves as a ballistic body.

The drag force on the body is given by

$$D = C_D S(\tfrac{1}{2}\rho V_T^2) \qquad [1]$$

Where C_D is the drag coefficient, S is the reference area upon which C_D is based, ρ is the air density, and V_T is the true velocity relative to the air (true airspeed). True airspeed is determined from inertial speed and wind speed as follows:

$$\vec{V}_T = \vec{V}_I - \vec{V}_W \qquad [2]$$

where the true airspeed ($\vec{V}_T$), inertial speed ($\vec{V}_I$), and wind speed ($\vec{V}_W$) are vector quantities.

The vector quantities in Equation [2] can be expressed in terms of components in a Cartesian axis system. Choosing this axis system to be fixed on the Earth with axes parallel to local lines of longitude and latitude, vector quantities can be expressed in terms of their North, East, and Vertical components:

$$\vec{V}_T = V_{TN}\hat{n} + V_{TE}\hat{e} + V_{TV}\hat{v} \qquad [3]$$

$$\vec{V}_I = V_{IN}\hat{n} + V_{IE}\hat{e} + V_{IV}\hat{v} \qquad [4]$$

$$\vec{V}_W = V_{WN}\hat{n} + V_{WE}\hat{e} + V_{WV}\hat{v} \qquad [5]$$

where the subscripts N, E, and V designate components in the North, East, and Vertical axes, and $\hat{n}, \hat{e}$, and $\hat{v}$ are unit vectors in the North, East, and Vertical directions, respectively. Positive values in the vertical axis are downward towards the center of the Earth.

From Equations [2] and [3-5] it follows that

$$V_{TN} = V_{IN} - V_{WN} \qquad [6a]$$

$$V_{TE} = V_{IE} - V_{WE} \qquad [6b]$$

$$V_{TV} = V_{IV} - V_{WV} \qquad [6c]$$

The total airspeed, V_T, and "horizontal airspeed," V_{TH}, are given by

$$V_T = \sqrt{V_{TN}^2 + V_{TE}^2 + V_{TV}^2} \qquad [7]$$

$$V_{TH} = \sqrt{V_{TN}^2 + V_{TE}^2} \qquad [8]$$

The rates of change of a ballistic object's inertial velocity components along the North, East, and Vertical axes are given by

$$m\frac{dV_{IN}}{dt} = -D_N = -C_D S\left(\frac{1}{2}\rho V_T^2\right)\left(\frac{V_{TN}}{V_{TH}}\right)\left(\frac{V_{TH}}{V_T}\right) = -C_D S\left(\frac{1}{2}\rho V_T^2\right)\left(\frac{V_{TN}}{V_T}\right) \qquad [9a]$$

$$m\frac{dV_{IE}}{dt} = -D_E = -C_D S\left(\frac{1}{2}\rho V_T^2\right)\left(\frac{V_{TE}}{V_{TH}}\right)\left(\frac{V_{TH}}{V_T}\right) = -C_D S\left(\frac{1}{2}\rho V_T^2\right)\left(\frac{V_{TE}}{V_T}\right) \qquad [9b]$$

$$m\frac{dV_{IV}}{dt} = W - D_V = mg - C_D S\left(\frac{1}{2}\rho V_T^2\right)\left(\frac{V_{TV}}{V_T}\right) \qquad [9c]$$

where D_N, D_E, and D_V are the components of the drag vector:

$$\bar{D} = D_N\hat{n} + D_E\hat{e} + D_V\hat{v} \qquad [10]$$

In Equations [9a-9c], m is the mass of the object, W is its weight, g is the acceleration due to gravity, and t is time. Note that weight only acts along the vertical axis. Rearranging Equations [9a-9c], we have

$$\frac{dV_{IN}}{dt} = -g\left(\frac{C_D S}{W}\right)\left(\frac{1}{2}\rho V_T^2\right)\left(\frac{V_{TN}}{V_T}\right) \qquad [11a]$$

$$\frac{dV_{IE}}{dt} = -g\left(\frac{C_D S}{W}\right)\left(\frac{1}{2}\rho V_T^2\right)\left(\frac{V_{TE}}{V_T}\right) \qquad [11b]$$

$$\frac{dV_{IV}}{dt} = g\left[1-\left(\frac{C_D S}{W}\right)\left(\frac{1}{2}\rho V_T^2\right)\left(\frac{V_{TV}}{V_T}\right)\right] \qquad [11c]$$

The trajectory of the ballistic object can be determined by double integration of Equations [11a-11c]. Note that these Equations all contain the term

$$\left(\frac{C_D S}{W}\right) = \left(\frac{W}{C_D S}\right)^{-1}$$

$W/(C_D S)$ is called the *ballistic coefficient* of the object. To determine the ballistic coefficient of a PW4000 engine separating from MSR990, the engine was treated as a cylinder, with a C_D of 0.9 along both the longitudinal and transverse axes. The value of the exposed area S depends on whether the cylinder is traveling along its longitudinal or transverse axis. Using a cylinder of radius = 5 ft. and length = 20 ft., and weighing 11,500 lb., the ballistic coefficients for the cylinder traveling along its longitudinal and transverse axes are:

$$\frac{W}{C_D S} = \frac{11{,}500\text{ lb.}}{(0.9)\pi(5\text{ ft})^2} \cong 163\text{ lb/ft}^2 \quad \text{(along longitudinal axis)} \qquad [12a]$$

$$\frac{W}{C_D S} = \frac{11{,}500\text{ lb.}}{(0.9)(10\text{ ft})(20\text{ ft})} \cong 64\text{ lb/ft}^2 \quad \text{(along transverse axis)} \qquad [12b]$$

Figure 1 shows the locations on the ocean surface where a ballistic object would fall, if released from MSR990 at five points along the airplane's flight path. For each release point, the impact location is shown for three values of $W/(C_D S)$: 64 lb/ft^2, 163 lb/ft^2, and the average of these, 114 lb/ft^2.

The initial velocity (both magnitude and direction) of the ballistic object is given by the flight conditions at the release point. The relevant parameters – horizontal position, altitude, ground speed, heading, and flight path angle – can be determined from the line in Figure 1 showing the flight path of MSR990, and from the table at the bottom of the Figure. The flight path shown in Figure 1 is the result of the curve fit through the radar data for this portion of the flight, as described in the Aircraft Performance Study.

The winds used in the trajectory calculations were those recorded by a radiosonde balloon released from Chatham, MA, at 1200 UTC on 10/31/1999. The values of wind direction and velocity as a function of altitude are shown in the table on the right side of Figure 1.

The engine release points along the MSR990 flight path are indicated by the black symbols in Figure 1. Symbols of different shapes are used for each release point. The points at which the engine impacts the ocean surface are shown by the colored symbols; the shape of each colored symbol is identical to that of its corresponding release point, and the different colors identify the value of the ballistic coefficient corresponding to each impact point. Thus, Figure 1 indicates that the higher the ballistic coefficient, the further the engine travels from its release point.

E. CONCLUSIONS

The engine impact points shown in Figure 1 indicate that it is unlikely that the left engine separated from MSR990 during the first dive or during the climb up to 24,000 ft. The impact points corresponding to an engine separation at 24,000 ft. are close to the debris field in which the left engine was found; however, at 24,000 ft., the airplane was near the top of its climb and at a relatively low airspeed and load factor. Hence, it is unlikely that the loads on the airplane would have caused an engine separation at this point, since the engine did not separate during much higher loading conditions during the first dive. No calculations were performed for separation points corresponding to the second and final dive of MSR990 because of the sparse and uncertain radar data during this time. However, the proximity of the airplane during the final dive to the debris fields and the high airspeeds that must have been encountered make it most likely that the engine separation occurred during this second dive.

[redacted]

John O'Callaghan
Senior Aerospace Engineer

EgyptAir Flight 990
Left Engine Impact Locations Assuming Various Separation Points

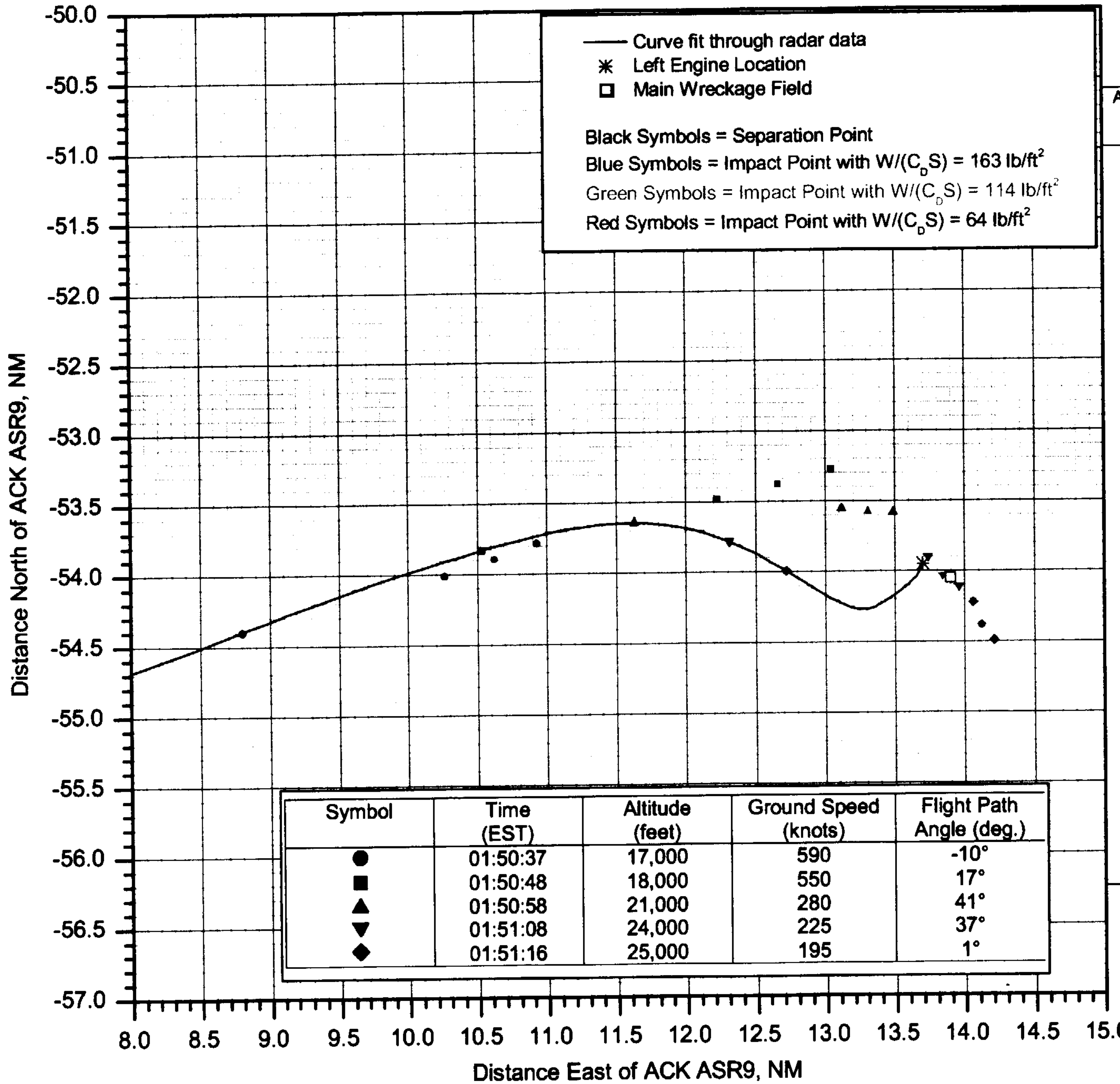

Symbol	Time (EST)	Altitude (feet)	Ground Speed (knots)	Flight Path Angle (deg.)
●	01:50:37	17,000	590	-10°
■	01:50:48	18,000	550	17°
▲	01:50:58	21,000	280	41°
▼	01:51:08	24,000	225	37°
◆	01:51:16	25,000	195	1°

Altitude (feet)	Wind Direction (True Deg.)	Wind Speed (knots)
-346	210	15.0
171	217	20.8
364	220	22.9
594	225	26.8
1589	230	24.9
2178	237	27.5
2441	239	28.7
2500	240	28.9
2579	240	28.9
2736	240	29.7
2795	240	30.0
3183	240	31.9
3566	240	33.8
4781	235	33.8
5530	235	32.8
6065	241	32.3
6461	245	31.9
6507	245	31.9
6861	247	31.5
7130	248	31.2
7487	250	30.9
8463	260	28.9
9010	262	27.0
9516	264	25.2
9883	265	23.9
11400	270	28.0
12573	270	29.7
13349	270	30.9
13634	272	30.9
15307	285	30.9
16007	284	33.0
18226	280	39.8
18289	280	38.9
18777	280	38.9
19213	280	38.9
23575	265	26.8
24096	260	24.9
24940	262	26.8
29040	270	35.9

Figure 1.